Aspects of Fabrication and Characterization of electro-thermal micro actuators

Paulo Henrique de Godoy
Polytechnic School of the University of Sao Paulo – Department of Mechatronics and Mechanical System Engineering - Av. Prof. Mello Moraes, 2231; São Paulo – SP, 05508-900, Brazil
pegodoy@uol.com.br

Emílio Carlos Nelli Silva
Polytechnic School of the University of Sao Paulo - Department of Mechatronics and Mechanical System Engineering - Av. Prof. Mello Moraes, 2231; São Paulo – SP, 05508-900, Brazil
ecnsilva@usp.br

Abstract: Simple thermal micro-actuators with a well-known behavior were considered in this study. This work describes a methodology and some of its important aspects to develop these electro-thermal micro-actuators. The core of the applied methodology is the use of the finite element method applied to a spiral of design process that allows us to predict the behavior of the micro-actuators before fabrication. To be correctly applied, this methodology required a sensitivity study of materials properties. The computational model is adjusted based on performed measurements of force and displacement. To evaluate the procedure these micro-actuators had their initial behavior characterized by finite element method using the commercial software ANSYS. The structural material used was the metallic nickel, plated at about 1 µm/min. The experimental characterization was carried out in a micro probe station with a CCD camera attached to it and a controlled voltage source. Among the results are the strong need of using FEM with a more accurate thermal and mechanical properties of the structural material (variation of its properties along with temperature) and a careful use of the thermal boundary conditions and the effects of heat convection and radiation, due to some deviations among experimental results and FEM results.

Keywords: Electro-thermo-mechanical MEMS, micro actuators, FEM simulation, force measurement, displacement measurement

1. Introduction

Micro-electromechanical Systems (simply MEMS in EUA) or MicroSystems Technology (simply MST in Europe and Asia) consists in mechanical micro-components (mobile or not) whose dimensions can stand among hundreds of microns and a few millimeters. Such micro-systems can be integrated with the microelectronic circuitry (such as accelerometers and pressure sensors) or not (such as valves and inkjet heads) (Petersen 1982, Rai-Choudhury 2000, Ishihara et al. 1996).

This research has focused studies on micro-actuators whose main purpose is to produce an action in the system they are therein. To perform the actuation, these microstructures need to be driven. Among the possibilities of driving a micro-actuator we can cite: capacitive or electrostatic, piezoelectric, electro-thermo-mechanic, magnetic, and by shape memory alloys (SMA). The first three are the most common. The electrothermomechanic way has advantages such as linearity between applied voltage and resulted displacement, higher force (compared to a capacitive drive), but a higher response time when compared to the other two most common. (Rai-Choudhury 2000, Ishihara et al. 1996; Jonsmann 2000; Mankame et.al. 2001; Que et.al. 2001). Another point is that no special or "exotic" material is needed to perform the actuation, making the fabrication step comparatively easy. Electro-thermo-mechanical micro actuators (or simply ETM micro actuators) work on the basic principle that thermal expansion of their elastic structure will produce displacement. This thermal energy is supplied to the system by the electrical resistance when an electric current flows through the structure (Joule effect). If the micro structure is properly anchored to a substrate, then a generation of mechanical strain will occur causing the displacement possible. Among the many possibilities of the ETM micro-actuator application (such as micropositioner, microgripper, microrelay, micromotor, microswitch) those applications that combine great demand for in-plane force with minimal chip-area are the most promising (Que et.al. 2001, Sinclair 2000).

The fabrication of these microstructures is complicated, comprising high cost materials and being time-demanding. The overall process based on a try-and-error systematic approach can take too long with no guarantee of satisfactory results. Thinking about these aspects, the development of new microsystems clearly needs to be performed under an integrated approach. In addition, this integrated approach can diminish the number of prototypes lowering costs. Thus, the concept of a spiral of process design was applied and it consists in five single steps: (i) design, (ii) computational simulation (predicting its initial behavior), (iii) physical implementation (fabrication), (iv) characterization, and (v) evaluation of the computer model based on real properties. By presenting these aspects, such as for example some particularities at computational modeling, we can contribute to build a roadmap for microstructures development. Normally these aspects are not well-presented on publications and they can take some time to be exactly clarified.

This article comprehends a complete description of each process phase with faced problems and adopted solutions in section 2. In section 3 a sensitivity study about materials properties in the ETM performance is presented. Section 4 enclosures the final conclusions of this work. Section 5 and section 6 end this work presenting the supporting institutions and the employed bibliography, respectively.

2. The overall procedures of the microstructures design and fabrication

The whole process of design and fabrication can be summarized in Figure 1. (i) The micro actuator is designed using CAD and the geometrical characteristics are defined; (ii) Finite Element Analysis is performed; (iii) the mask lay-out is carried out using the technique with the most attractive cost - photolite; (iv) fabrication of the micro structures onto substrates such as alumina and silicon by electroplating technique (copper, nickel, some alloys); (v) wet stripping of sacrificial layers is applied to finish the prototypes; (vi) experimental characterization of displacement and blocking force, and electrical resistivity; (vii) re-evaluation of the computational model based on experimental data.
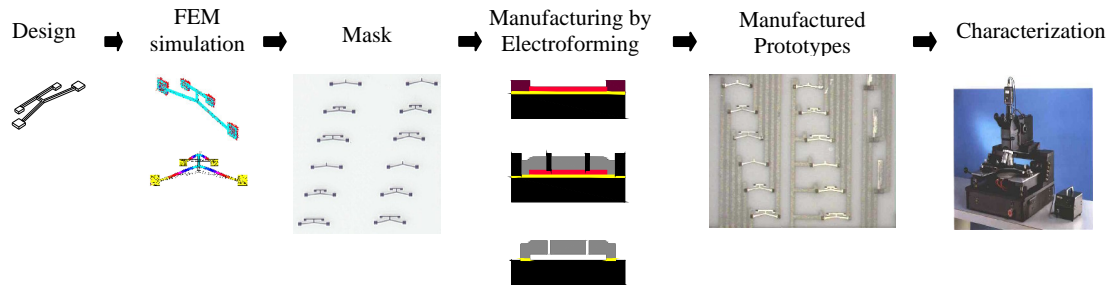
Design ➡ FEM simulation ➡ Mask ➡ Manufacturing by Electroforming ➡ Manufactured Prototypes ➡ Characterization

Figure 1. The overall process for micro-system development.

2.1. Designing the micro-actuators.

Essentially microactuators can be designed by using two distinct approaches: (i) a systematic methodology, called topology optimization, and (ii) a trial-and-error concept, the so called "intuitive" design. The topological optimization (TOpt) methodology basically distributes the material in an initial and fixed domain, discretized in finite elements, to extremize a cost function. The trial-and-error concept means a process involving successive design, fabrication and characterization steps of the structure. The results are evaluated, and the process starts again (design modification, fabrication and characterization). This procedure will be repeated until the satisfactory result (so-called "optimal" shape) can be obtained. This process takes too long; however, it uses simple geometric shapes. In this work, "intuitive" actuators are considered to be a union of simple shapes. Topology Optimization generates complex shapes and once the objective of this work is to evaluate the application of a systematic approach on the development of structures focusing on the influence of material properties on their performance, this research work used the measurement of microactuators with simple design based on some well-established concepts (Que et.al. 1999; Park et.al. 2000; Chu et.al. 2003). Figure 2 shows a micro-actuator with an opened-"V" geometry in two possible design conditions. These micro-actuators have a line width of 50 microns, and the anchor pads are squares of 250. In Figure 2c, it can be seen a spring attached to the micro-actuators. The function of the spring is to collect the force data indirectly through its deformation. The spring behavior (rigid) was calculated by FEM analysis to block the micro-actuator displacement at maximum work.
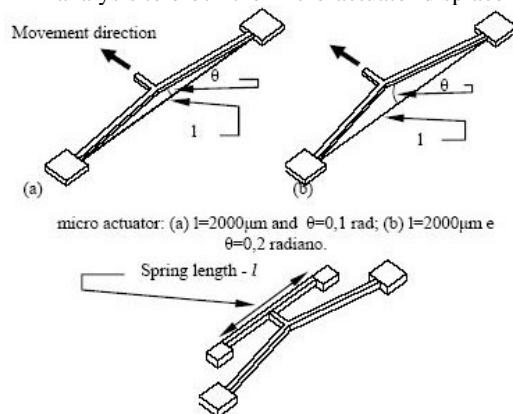
Movement direction

micro actuator: (a) l=2000μm and θ=0,1 rad; (b) l=2000μm e θ=0,2 radiano.

Spring length - l

Figure 2. ETM micro-actuators with unidirectional movements. (a,b) without spring, (c) with attached spring.

2.2. Modeling the microstructures by Finite Element Method (FEM).

The FEM analysis of micro-actuators was carried out by using the ANSYS software which has some specific elements for MEMS simulation. In these analysis the correct application of the boundary conditions and material properties are very important for the final result.

On the modeling implementation, the input parameters are vectors of nodal temperature and nodal voltage, vector of surface forces (natural convection) and material physical properties. The Eq. (1) showed below is solved by ANSYS for displacement, current density, and temperature gradient.

$$
\begin{bmatrix} [M] & [0] & [0] \\ [0] & [0] & [0] \\ [0] & [0] & [0] \end{bmatrix} \begin{Bmatrix} \{\ddot{u}\} \\ \{\ddot{T}\} \\ \{\ddot{V}\} \end{Bmatrix} + \begin{bmatrix} [C] & [0] & [0] \\ [0] & [C^t] & [0] \\ [0] & [0] & [0] \end{bmatrix} \begin{Bmatrix} \{\dot{u}\} \\ \{\dot{T}\} \\ \{\dot{V}\} \end{Bmatrix} + \begin{bmatrix} [K] & [0] & [0] \\ [0] & [K^t] & [0] \\ [0] & [0] & [K^v] \end{bmatrix} \begin{Bmatrix} \{u\} \\ \{T\} \\ \{V\} \end{Bmatrix} = \begin{Bmatrix} \{F\} \\ \{Q\} \\ \{I\} \end{Bmatrix}
$$

(1)

Where:

      [Kt] = [Ktb] + [Ktc]
      {Q} = {Qnd} + {Qc} + {Qg} + {Qj}
      {I} = {Ind}
      {F}={Fnd}+{Fth}+{Fpr}

The FEM analysis in ANSYS employs an element named SOLID98, which has tetrahedral shape with 10 nodes (appropriated for irregular meshes). The analysis can be carried out considering coupled (single step) or uncoupled (multi-step) multi-physics environment. The choice between them will depend on the operational conditions of micro-actuators. The single step is considerably easier to be used and the large displacement feature was not required because the simulated displacement was larger than the experimental one (section 3).

Considering the boundary conditions, the correct application of the voltage and the thermal boundary conditions are important because they can affect the final result considerably. The voltage was applied to the central node of the mechanical anchor (electrical pad). Thermal boundary condition can be applied by two forms: (i) imposing the environmental temperature right at the bottom of the mechanical anchors (called "essential thermal boundary condition" or ETBC); and (ii) imposing the environmental temperature at the substrate (called "natural thermal boundary condition" or NTBC). The NTBC must be used in structures whose thermal dissipation is not ideal at substrate. This condition increases the overall energetic efficiency of the microactuator (Mankame et.al., 2001). This condition leads to a more accurate result for displacement/current, however, has higher solution time because the substrate must be also simulated. In this work the ETBC condition was used to reduce the solution time.

The material properties together with thermal boundary conditions are the most important factors that affect the simulation results. Table 1 summarizes the properties used for the initial modeling of the structures (Structural material nickel). Young modulus and thermal expansion coefficient were obtained on Jonsmann (2001), and all other properties came from Lide (1998).

Table 1. Nickel Material's property.

Nickel										
E*		188 GPa								
ν		0.31								
α*		15 ppm/K								
density		8908 g/cm^3								

T	(K)	250	300	350	400	500	600	800	1000	1200	1400
Kx	(W/mK)	97.5	90.7	85	80.2	72.2	65.6	67.9	71.8	76.2	80.4
T	(K)	273	293	298	300	400	500	600	700	800	900
ρ	(μΩ.cm)	6.16	6.93	7.12	7.2	11.8	17.7	25.5	32.1	35.5	39.6

2.3. The fabrication technique.

The fabrication technique used here (Madou 1997) combines UV-lithography, electroplating of copper and nickel and selective etching. The UV-lithography consists of patterning a photopolymer layer by UV light to form a mold. This mold area is delimited by lithographic masks. Normally the size of the minimal aspects defines the type of the lithographic mask. Masks with minimal aspect of 1 to 10 microns necessarily makes use of processes that have high production cost (such as e-beam). In the case of this work, the chosen type of lithographic mask has a line resolution of 30-40 microns. It has low cost, however, it has the poorest quality (the mask has many pores and a line roughness factor –rugosity- of 2 to 3 microns).

The micro-actuators were fabricated by electroplating technology applying nickel as structural material and copper as sacrificial layer. Figure 3 shows a schematic diagram used on the process. The apparatus for metal plating consists of a 2000 ml glass Becker over a hot plate (used on nickel bath), a current source, an amp meter, a stir, an anode made of copper (copper bath) or NiP (nickel bath) and a sample holder.

There were used two different bath compositions for the structural material: baths with additives and baths without additives. The additives are organic substances that are used for grain refining, uniformization of the deposits, reducing internal stress, and giving brilliance to the metal.

As these structures are supposed to be mobile, a sacrificial layer must be grown. The easy strip of sacrificial layer is an important variable to take into account when choosing the sacrificial layer material. The material used as a sacrificial layer in this case was copper because of the easy selective-stripping to nickel (hydrogen peroxide, ammoniac and de-ionized water 1:1:3). Other options could exist for sacrificial layer material such as the use of photo resists. However, in that case, the mask quality must be good enough and the pos-cure parameters (temperature-time) appropriate in order to prevent blister formation. There were used additives for grain refining and increasing the film´ brilliance.
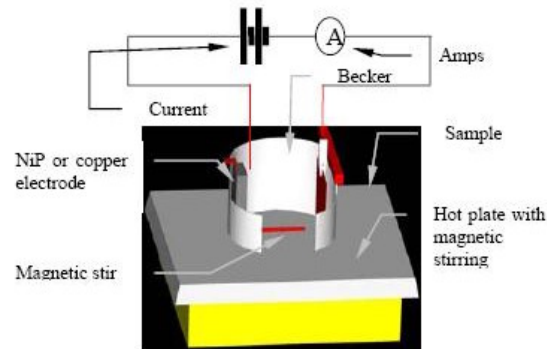

Figure 3. Schematic drawing of the electroplating process.

The overall process is described below:

i.   The substrate consists of an alumina plate (2 square inches) with a seed layer of titanium (0,02 microns) and gold (0,2 microns);
ii. pattern a sacrificial layer mold. As the height of this layer is of about 6-12 microns, the photo resist choice was AZ-4620 of Clariant. This photo resist is of easy strip (ketone);
iii. Next, Copper is electroformed for the sacrificial layer;
iv. Remove the polymer layer and rinse the sample with Copper persulphate to eliminate oxide on the copper layer;
v.   Spin the negative polymer (SU-8) with 45 to 60 microns. Proceed with the mask align (sacrificial and structural layer) and expose to UV light;
vi. Electroform the structural layer with nickel;
vii. Finally, remove SU-8 mould, sacrificial layer, and seed layer with appropriate baths.

2.4. The characterization step

To characterize the micro actuator, firstly it was necessary to determine how the electric power would be applied to the system. The two possibilities of electrical power control were: (i) control by voltage, and (ii) control by current. It was observed in calculations that if a control by current is employed, a point of electrical instability could take place. In this case, it was employed the electrical power control by voltage.

The experimental characterization consists in applying a voltage to the micro-actuator, then obtaining the resultant current data and finally capturing an image of the micro-actuator after movement (if so). The voltage application began on 50 mV, later to 100mV, and kept going on 100 to 100 mV until 1.7 V. With the voltage and current data obtained, the resistivity of the employed metal was calculated.

3. Results and Discussion

3.1. Sensitivity study.

The sensitivity study was conducted on physical properties of the structural material (nickel). This was important to determine the most relevant property of micro-actuator behavior. First study relied on natural thermal convection. Mankame et.al (2001) and Jonsmann (2000) have already been shown the relevance of this property. They mentioned that its experimental derivation is too difficult in this scale. Thus, thermal convection coefficient must be inferred and this can lead to significant errors. However, how could be its influence? Well, making some parameters constant (293K on the anchor, 1400 mV of driven voltage, and structure height of 28 microns), the influence of a thermal convection coefficient change on actuator behavior could be noted. Table 2 summarizes the analysis.

Table 2. Sensitivity test of the natural thermal convection coefficient.

h (W/m²K)	Uy (μm)	T (K)	I (mA)
0	414.0	8117.0	2436.8
5000	100.0	1961.0	2499.1
18700	37.1	926.3	2709.4
33000	25.7	741.4	3200.0
55000	nc	nc	nc

Between the two most common values (18700 and 33000) in the literature, the obtained discrepancy on displacement (Uy) was about 50%. Observing initial values, the discrepancy was even higher. Another analysis was the number of areas being considered on the model that are able to contribute to heat exchange to environment. Three situations were considered (contact areas were not used): all external areas (A1); all external areas but anchor areas (A2), all external areas but anchor areas and areas on the moving structure close to the substrate (A3). 30% less displacement was observed when the areas close to the substrate were neglected. Considering mesh refinement, there was no significant deviation on displacement results but stronger computational work.

Second study was to observe the influence of physical properties of nickel (young modulus, thermal expansion coefficient, electrical resistivity and thermal conductivity). To perform this, the natural thermal convection coefficient was locked at 18700 W/m^2 (experimental data obtained by Jonsmann 2000) and all areas but anchors exchange heat to environment.

No significant deviation was observed for any variation of young modulus. For thermal expansion coefficient change of 10.5% around base value (that obtained by Jonsmann 2000), a 10.67% deviation was obtained. Diminishing the value, the thermal expansion coefficient diminishes too; increasing the value, the coefficient increases too. Thermal conductivity coefficient is a temperature-dependent property. There is a tabled valued for nickel on Lide (1998). However, it is well known that material behavior is different from micro to macro environment mainly because processing techniques (Askeland 1996). Assuming that there is no discrepancy among values, two new tables there were prepared varying ±15% around base value. Table 3 shows the calculated values.

Table 3. Thermal conductivity coefficient.

			250	300	350	400	500	600	800	1000	1200	1400
*	T	(K)	250	300	350	400	500	600	800	1000	1200	1400
	Kx	(W/mK)	97.50	90.70	85.00	80.20	72.20	65.60	67.90	71.80	76.20	80.40
*1	T	(K)	250	300	350	400	500	600	800	1000	1200	1400
	Kx	(W/mK)	112.13	104.31	97.75	92.23	83.03	75.44	78.09	82.57	87.63	92.46
*2	T	(K)	250	300	350	400	500	600	800	1000	1200	1400
	Kx	(W/mK)	82.88	77.10	72.25	68.17	61.37	55.76	57.72	61.03	67.77	68.34

*   Original temperature table.
*1   15% high temperature table.
*2   15% lower temperature table.

Based on these tables it was found a deviation on displacement of -1.08% for lower values and +1.33% for higher values.

Electrical resistivity also changes with. Thus, two new tables concerning a variation of ±15% around base value was prepared. Table 4 resumes these values.

Table 4. Electrical resistivity property values.

			273	293	298	300	400	500	600	700	800	900
*	T	(K)	273	293	298	300	400	500	600	700	800	900
	ρ	(μΩ.cm)	6.16	6.93	7.12	7.20	11.8	17.7	25.5	32.1	35.5	39.6
*1	T	(K)	273	293	298	300	400	500	600	700	800	900
	ρ	(μΩ.cm)	8.01	9.01	9.26	9.36	15.3	23.0	33.2	41.7	46.2	50.2
*2	T	(K)	273	293	298	300	400	500	600	700	800	900
	ρ	(μΩ.cm)	4.31	4.85	4.98	5.04	8.26	12.4	17.9	22.5	24.9	27.0

*   Original temperature table.
*1   30% high temperature table.
*2   30% lower temperature table.

For a 30% change on property value, there was a variation of -11.3% and +30.0% on displacement; -6.4% and +22.2% on temperature, and finally -14.9% and 28.0% on electrical current.

3.2. Experimental data.

As shown in the Figure 4, the plating solution has a strong influence over the electrodeposited nickel properties (electrical resistivity). The nickel plated from the plating solution containing additives became more resistive than the plating solution without it.
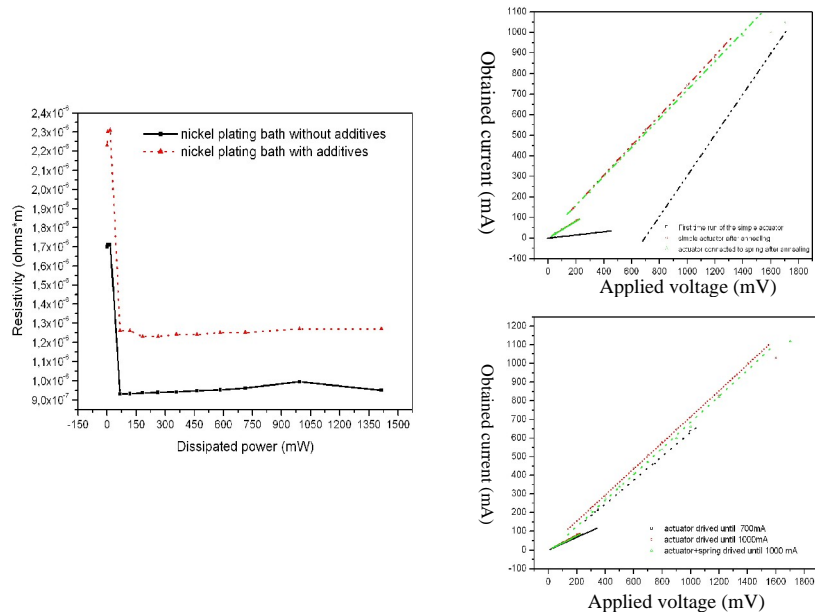
Figure 4. Resistivity of the plating solutions on the micro actuators.

Also in the Figure 4, it is shown how the electrical current can vary along with the applied voltage. Two different inclinations on each line can be noted that is supposed to be independent on the metal kind.

Another differentiation on metal resistivity along with the temperature can be seen. This complication on the characterization step occurred with the increasing thermal energy in the system. The values of the obtained current had visible variation from one cycle to another. A possible answer for this fact could be a physical change in the plated metal. According to these observations, it was determinate that all structures, prior to the characterization step would be annealed in some temperature close to the maximum operating temperature. The maximum operational temperature was fixed to be at 623 K to avoid oxide formation over the micro-actuator surface.

The blocking force was determined indirectly by calculations using the spring constant attached to the micro actuator and the maximum displacement obtained. The result is plotted at the Figure 5.

(a)

Measured displacement X estimated
working-temperature
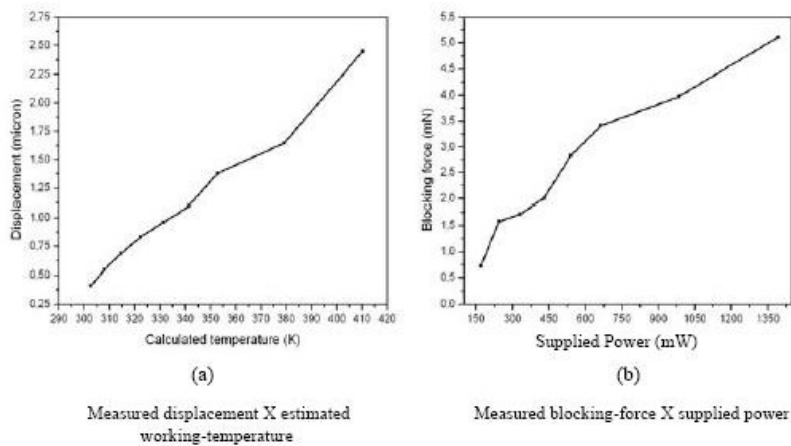
(b)

Measured blocking-force X supplied power

Figure 5. Blocking-force and estimated working-temperature.

Figure 6 demonstrates the present methodology for the displacement characterization. The obtained values for these parameters on alumina and silicon substrates are indicated therein.
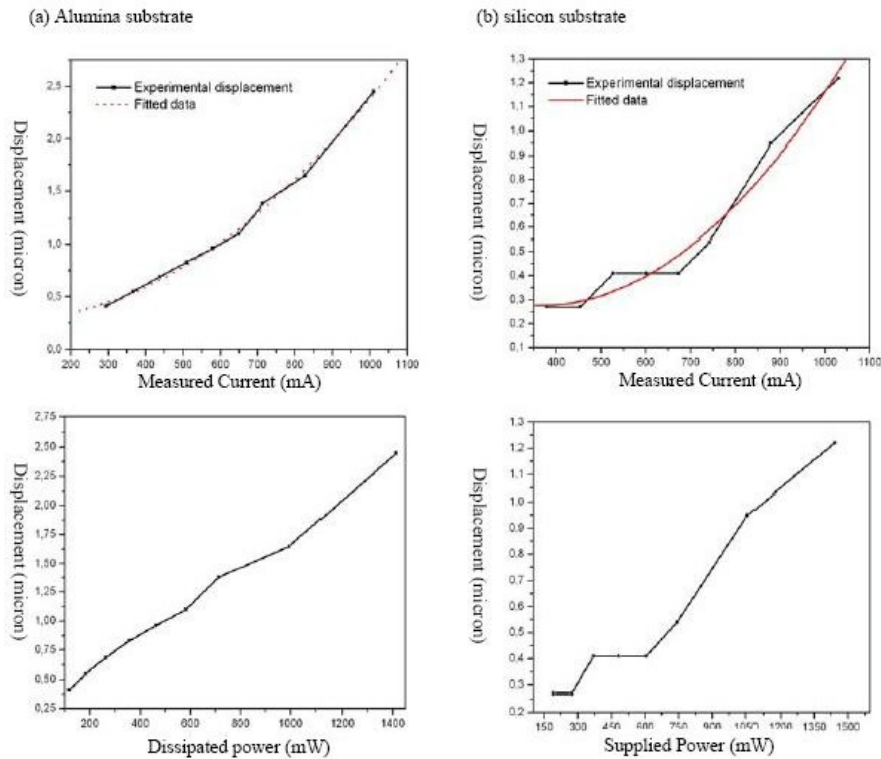
Figure 6. Experimental data for two different kind of substrate.

3.3. Feedback for the computational model

The complete cycle for the micro-actuator implementation comprehend a feedback of the experimental data to the computational model to make the computational model more realistic by improving the time for a micro-actuator final release. In this case, the computational model firstly used material properties obtained from literature. However, the plated material has strong influence on the electroplating conditions and additives employed. The first results showed a big difference from the experimentally obtained displacement and the computationally obtained displacement. From the measurement of the plated nickel resistivity, the model starts to converge along with the experimental data.

Two comparisons could be made: one points to the electrical current and another points to the displacement. The computational and experimental data obtained for the electrical current points to no more than 3% of deviation. Although the data for displacement points for large deviations between two curves, the computational model must still be improved, because there can exist more variables influencing. Among these variables, thermal conductivity and thermal expansion coefficient can make some influence on the thermal distribution on the micro-actuator causing a difference on the displacement value.
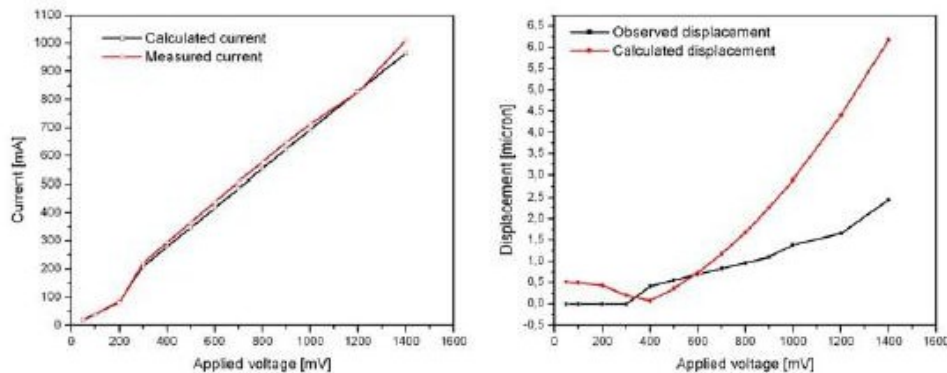

Figure 7. Comparison between computational model and experimental data.

4. Summary

The conducted work on computational modeling and experimental characterization contributed to start the understanding the role of the substrate on the displacement of these ETM micro-actuators. Also this work establishes the full cycle of micro-actuator design process, involving a computational simulation, fabrication, characterization, and the feedback step.

More work can be conducted on the material properties and microstructure. Also some tries would be done on the temperature quantification.

5. Acknowledgements

6. References

Askeland, D.R.. The Science & Engineering of Materials Solutions Manual. New York: Chapman & Hall, 1996. 408p. ISBN 0412726106.

Bendsøe, M. P., "Optimization of Structural Topology, Shape, and Material", Springer, Berlin, 1995.

Chu, L.L.; and Gianchandani, Y.B.; "Amicromachined 2D positioner with electrothermal actuation and sub-nanometer capacitive sensing"; J. Micromech. Microeng. N.13 pp.279–285 (2003).

Ishihara, H., Arai, F. e Fukuda, T., "Micro Mechatronics and Micro Actuators", IEEE/ASME Transactions on Mechatronics, vol. 1, nº. 1, p. 68-79, 1996.

Jonsmann, J.; "Technology development for topology optimized thermal microactuators", PhD thesis, The Microelectronics Centre, Technical University of Denmark, pp.116, 2000.

Lide, D.R., 1998, "CRC Handbook of Chemistry and Physics", Publisher: CRC Press. 79th edition. 2496 p. ISBN: 0849304792.

Madou, M. J., "Fundamentals of Microfabrication", CRC Press, EUA, 1997.

Mankame, ND; and Ananthasuresh, GK; "Comprehensive thermal modeling and characterization of an electro-thermal-compliant microactuator"; J. Micromech. MicroEng. V.11, pp.452-462, 2001.

Park, J-S; Chu, LL; Siwapornsathain, E; and Gianchandani, YB; "Long throw and rotary output electro-thermal actuators based on bent-beam suspensions"; IEEE International Micro Electro Mechanical Systems Conference, Japan, pp.680-685, 2000.

Petersen, K; "Silicon as mechanical material"; Proc. IEEE Electron. Devices, 70(5), pp.420-457 (1982).

Que, L.; J.-S., Park, and Gianchandani, Y.B.; "Bent-Beam Electrothermal Actuators—Part I: Single Beam and Cascaded Devices"; Journal of Microelectromechanical Systems, v.10, n.2, 247-254, 2001.

Que, L; Park, J-S; Gianchandani, YB; "Bent-Beam Electro-Thermal Actuators for High Force Applications"; IEEE International Micro Electro Mechanical Systems Conference, Orlando, FL, pp.31-36, 1999.

Rai-Choudhury, P., 2000, "MEMS and MOEMS technology and applications", Ed. by SPIE-Press, 520 p., ISBN 0-8194-3716-6.

Sinclair, M.J., 2000, "A high force low area MEMS thermal actuator", In IEEE Proceedings of the Inter Society Conference on Thermal Phenomena. pp.127-132.

7. Nomenclature and superscripts.

Nomenclature.

[M]	Structural mass matrix;	{Fth}	thermal strain force vector;
[C]	Structural damping matrix;	{Fpr}	pressure load vector;
[Ct]	thermal specific heat matrix;	{Qnd}	applied nodal heat flow rae vector;
[K]	Structural stiffness matrix;	{Qc}	convection surface vector;
[Kt]	thermal conductivity matrix;	{Qg}	heat generation rate vector for causes other than Joule heating;
[Ktb]	thermal conductivity matrix of material;	{Qj}	heat generation rate vector for Joule heating;
[Ktc]	thermal conductivity matrix of convection surface;	{Ind}	applied nodal electric current vector;
[Kv]	electric coefficient matrix;	{u}	displacement vector;
{Fnd}	applied nodal force vector;	{T}	thermal potential (temperature) vector;
		{V}	electric potential vector;

Superscripts.
.   time derivative
. .   second time derivative